Investigation of electrochromic band-shifts in the Soret region induced by the formation of $Tyr_D^{\bullet}$, $Tyr_Z^{\bullet}$, and $Q_A^{\bullet -}$ in Photosystem II.

Alain Boussac*[1], Takumi Noguchi[2], A. William Rutherford[3], Julien Sellés[4], Miwa Sugiura[5], Stefania Viola[6].

The authors are given in alphabetic order

*Corresponding author

[1]Institut de Biologie Intégrative de la Cellule, UMR9198, CEA Saclay, 91191 Gif-Sur-Yvette, France. alain.boussac@laposte.net

[2]Department of Physics, Graduate School of Science, Nagoya University, Furo-cho, Chikusa-ku, Nagoya 464-8602, Japan. tnoguchi@bio.phys.nagoya-u.ac.jp

[3]Department of Life Sciences, Imperial College, SW7 2AZ London, UK. a.rutherford@imperial.ac.uk

[4]Institut de Biologie Physico-Chimique, UMR CNRS 7141 and Sorbonne Université, 13 rue Pierre et Marie Curie, 75005 Paris, France. selles@ibpc.fr

[5]Proteo-Science Research Center, and Department of Chemistry, Graduate School of Science and Technology, Ehime University, Bunkyo-cho, Matsuyama, Ehime 790-8577, Japan. miwa.sugiura@ehime-u.ac.jp

[6]Institute of Biosciences and Biotechnologies of Aix-Marseille – UMR7265, Saint-Paul-Lez-Durance, France. stefania.viola@cea.fr

ORCID numbers:

Alain Boussac: 0000-0002-3441-3861

Takumi Noguchi: 0000-0002-3281-6827

A. William Rutherford: 0000-0002-3124-154X

Julien Sellés: 0000-0001-9262-8257

Miwa Sugiura: 0000-0002-4232-5941

Stefania Viola: 0000-0003-0773-8158

Abstract

The effects of $Tyr_D^{\bullet}$, $Tyr_Z^{\bullet}$, and $Q_A^{\bullet-}$ radical formation on the absorption spectrum in the Soret region were studied in Mn-depleted Photosystem II at pH 8.6 (in order to be in the Tyr_D state after the dark adaptation). Flash-induced difference spectra were recorded in several PSII samples from *i*) *Thermosynechococcus vestitus* (formerly *T. elongatus*), *ii*) *Synechocystis* sp. PCC 6803, *iii*) *Chroococcidiopsis thermalis* PCC7203 grown under far-red light, and *iv*) *Acaryochloris marina*. In the case of *T. vestitus*, mutants D1/H198Q, D1/T1789H, D2/I178H and D2/Y160F, with PsbA1/Q130 instead of PsbA3/E130, were also studied for possible contributions from P_{D1}, Chl_{D1}, Chl_{D2} and Phe_{D1}, respectively. For a possible contribution from P_{D2}, the D2/H197A mutant was studied in *S*. 6803. While P_{D1} is clearly the species whose spectrum is blue shifted by ~ 3 nm in the presence of $Q_A^{\bullet-}$, as already well documented in the literature, the species whose spectra are shifted upon the formation of $Tyr_D^{\bullet}$, and $Tyr_Z^{\bullet}$ remain to be clearly identified as they appear different from P_{D1}, P_{D2}, Phe_{D1}, Chl_{D1} and Chl_{D2} as concluded by the lack of different light-induced difference spectra in the mutants listed above. Although we cannot rule out too weak effect taking into account the accuracy of the experiments, it is proposed that other pigments are involved as antenna Chl and/or Car near the reaction center. Additionally, it is shown that, *i*) there is no proton release into the bulk upon the oxidation of Tyr_D at pH 8.6, and *ii*) the rearrangement of the electrostatic environment of the pigments involved in the light-induced different spectra in the samples studied upon the formation $Tyr_D^{\bullet}$, $Tyr_Z^{\bullet}$, and $Q_A^{\bullet-}$ likely occur differently on a kinetic and structural point of views.

Introduction

Oxygenic photosynthesis in cyanobacteria, algae and higher plants converts solar energy into the chemical bonds of sugars and of dioxygen. Photosystem II (PSII) begins this process by splitting water to obtain electrons in the form of reduced quinones, while generating a proton gradient and releasing O_2. The mature PSII binds 35 chlorophylls *a* (Chl-*a*), 2 pheophytins (Phe-*a*), 1 membrane b-type cytochrome, 1 extrinsic c-type cytochrome (in cyanobacteria and red algae), 1 non-heme iron, 2 plastoquinones (Q_A and Q_B), the Mn_4CaO_5 cluster, 2 Cl^-, 12 carotenoids and 25 lipids [1,2]. In the cyanobacterium *Synechocystis sp.* PCC 6803 a 4th extrinsic subunit, PsbQ, has also been found in addition to PsbV, PsbO and PsbU [3].

Among the 35 Chl-*a*, 31 are antenna Chl's. When one is excited, the excitation energy is transferred to other chlorophylls until it reaches the key pigments in photochemical reaction centre [3]: 4 Chl-*a* molecules, P_{D1}, P_{D2}, Chl_{D1}, Chl_{D2} and 2 Phe-*a* molecules, Phe_{D1} and Phe_{D2}. A few picoseconds after the formation of the excited $^*Chl_{D1}$, a charge separation occurs resulting ultimately in the formation of the $Chl_{D1}^{\bullet+}Phe_{D1}^{\bullet-}$ and then $P_{D1}^{\bullet+}Phe_{D1}^{\bullet-}$ radical pair states [5,6]. Formation of the $Chl_{D1}^{\bullet+}Phe_{D1}^{\bullet-}$ radical pair was recently defined as a fast pathway (short-range charge-separation) in contrast with a slow pathway with $P_{D1}P_{D2}$ as the initial donor (long-range charge separation) that would result directly in the formation of the $P_{D1}^{\bullet+}Phe_{D1}^{\bullet-}$ radical pair [7].

After this charge separation, $P_{D1}^{\bullet+}$ oxidizes Tyr_Z, the Tyr161 of the D1 polypeptide, which then is reduced by the Mn_4CaO_5 cluster. The electron on $Phe_{D1}^{\bullet-}$ is then transferred to Q_A, the primary quinone electron acceptor, and then to Q_B, the second quinone electron acceptor. Whereas Q_A can be only singly reduced under normal conditions, Q_B accepts two electrons and two protons before to leave its binding site and to be replaced by an oxidized Q_B molecule from the membrane plastoquinone pool, see for example [8–12] for a non-exhaustive list of recent reviews on PSII function. The Mn_4CaO_5 cluster, oxidized by the $Tyr_Z^\bullet$ radical formed after each charge separation, cycles through five redox states denoted S_n, where n stands for the number of stored oxidizing equivalents. When the S_4-state is formed two water molecules bound to the cluster are oxidized, O_2 is released and the S_0-state is reformed [13,14].

Formation of the $Q_A^{\bullet-}$ species is known to induce spectral changes of Phe_{D1} in the Qx region around 550 nm [15-17], and of P_{D1} in the Qy region between 650 and 700 nm, *e.g.* [18,19]. These electrochromic responses have been extensively studied both experimentally

and theoretically [18,19]. For example, it has been observed that in the presence of $Q_A^{\bullet -}$ the blue shift of the Qy band of Chl_{D1} seen classically at ~ 680 nm was replaced by one at ~ 727 nm in Far Red Light PSII thus indicating that the Chl-*a* acting as the Chl_{D1} was replaced by a Far Red Light chlorophyll (likely a Chl-*d*) [20]. The Soret band of P_{D1} is also sensitive to the formation of $Q_A^{\bullet -}$ and to the charge in and around the Mn_4CaO_5 cluster [21,22]. That said, spectral changes in the blue are far less well studied than the Qx and the Qy bands, see however [18] For this reason, we report here an initial characterization of the spectral changes between 400 and 460 nm induced by the formation of the $Tyr_D^{\bullet}$, $Tyr_Z^{\bullet}$, and $Q_A^{\bullet -}$ radicals. In order to have the highest proportion of centers with a reduced Tyr_D after the dark-adaptation, and no contribution from the Mn_4CaO_5 cluster, the experiments were performed at pH 8.6 in several Mn-depleted PSII [23].

Materials and Methods

The PSII samples used were: *i*) the PsbA3-PSII [24], the PsbA3/H198Q mutant [25], the PsbA3/T179H mutant [26], the Tyr_D-less mutant (with D1 = PsbA1) [27], and the D2/I178H mutant (with D1 = PsbA3) [28], all purified from *Thermosynechococcus vestitus*, *ii*) the FRL-PSII from *Chroococcidiopsis thermalis* [20,29] with 4 Chl-*f* and 1 Chl-*d*, *iii*) the wild type and D2/H197A mutant from *Synechocystis* 6803 [30], and *iv*) PSII from *Acaryochloris marina* [29] with 34 Chl-*d* and 1 Chl-*a* at the P_{D1} position [31]. The samples were Mn-depleted by adding ~10 mM NH_2OH, from a stock at 1 M at pH 6.5, and 1 mM EDTA. The hydroxylamine was then removed by washing of the PSII samples by cycles of dilution in 1 M betaine, 15 mM $CaCl_2$, 15 mM $MgCl_2$, 100 mM Tris, 100 μM EDTA, pH 8.6 (adjusted with HCl), followed by concentration using Amicon Ultra-15 centrifugal filter units (cut-off 100 kDa), until the estimated residual NH_2OH concentration was lower than 0.1 μM in the concentrated PSII samples before the final dilution. In the final dilution step, the PSII samples were suspended in 1 M betaine, 15 mM $CaCl_2$, 15 mM $MgCl_2$, 100 mM Tris, pH 8.6. For the experiment reported in Fig. 8 the Tris buffer was replaced by the Mes buffer at pH 6.5.

For the measurements with the dye thymol blue the Mn-depleted Tyr_D-less PSII at pH 8.6 was washed by cycles of dilution in 100 mM NaCl, 15 mM $CaCl_2$, 15 mM $MgCl_2$, followed by concentration using Amicon Ultra-15 centrifugal filter units (cut-off 100 kDa), until the estimated residual Tris concentration was lower than 1 μM in the concentrated PSII samples before the final dilution. After dark adaptation for 3 to 4 hours at room temperature

150 µM thymol blue and 100 µM PPBQ (in dimethyl sulfoxide) were added. During measurement, the sample was continuously bubbled with ALPHAGAZ 2 Argon from Air Liquid, in which the CO_2 contamination is ≤ 0.1 ppm. This bubbling was performed to minimize the drift in the baseline (*i.e.* in the pH) due the solubilisation of atmospheric CO_2.

Time-resolved absorption changes measurements were performed with a lab-built spectrophotometer [32] modified as described in detail in [33]. The chlorophyll concentration of the samples was ~ 25 µg of Chl mL^{-1}.

Results and Discussion

Panel A in Fig. 1 shows the ΔI/I recorded at 432 nm in Mn-depleted PsbA3-PSII at pH 8.6 illuminated by 10 saturating flashes (spaced 2 s apart) in the presence of the electron acceptor PPBQ. The sample used was dark-adapted for 3 to 4 hours at room temperature before the flash illumination. Panel B shows a zoom of the data recorded after the first 4 flashes. In this experiment, the first weak, non-actinic, detector flash was given 200 µs after each of the actinic flashes. The second weak, non-actinic, detector flash was given 10 ms after each of the actinic flashes. Then, 20 weak, non-actinic, detector flashes (spaced 100 ms apart) were given after each of the 10 actinic flashes.

At pH 8.6, and after a long dark-adaptation, Tyr_D is reduced in the great majority of the centers. In these conditions the first actinic flash oxidizes either Tyr_D or Tyr_Z in almost equal proportion [23]. The non-decaying ΔI/I recorded 2 s after the first flash, black vertical arrow in Panel B of Fig. 1, is a consequence of $Tyr_D^{\bullet}$ formation alone since, 2 s after the flash, $Tyr_Z^{\bullet}$ and $Q_A^{\bullet-}$ are no longer present. Always after the first flash, the yellow vertical arrow, that is the 200µs-*minus*-10ms difference, corresponds to a mixing of the $Tyr_D^{\bullet}Q_A^{\bullet-}$-*minus*-$Tyr_D^{\bullet}Q_A$ and $Tyr_Z^{\bullet}Q_A^{\bullet-}$-*minus*-$Tyr_Z^{\bullet}Q_A$ differences. In other words, it is a mixing of the $Q_A^{\bullet-}$-*minus*-Q_A difference in the presence of either $Tyr_D^{\bullet}$ or $Tyr_Z^{\bullet}$. After the 4th flash, when $Tyr_D^{\bullet}$ was formed in virtually all centers, the flash illumination only induced the formation of the $Tyr_Z^{\bullet}Q_A^{\bullet-}$ state, and the slow decay in the s time range corresponds to the decay of $Tyr_Z^{\bullet}$. Consequently, the red vertical arrow that is the 200µs-*minus*-10ms difference corresponds to the $Tyr_Z^{\bullet}Q_A^{\bullet-}$-*minus*-$Tyr_Z^{\bullet}Q_A$ difference, in other words the $Q_A^{\bullet-}$-*minus*-Q_A difference in the presence of $Tyr_Z^{\bullet}$ and $Tyr_D^{\bullet}$. This differs from the first flash where the $Q_A^{\bullet-}$-*minus*-Q_A difference was measured is the presence of only one of the two tyrosyl radicals, either $Tyr_Z^{\bullet}$ or $Tyr_D^{\bullet}$. Always after the 4th flash, the violet vertical arrow, in Panel B of Fig.1, is the ΔI/I 200 µs after flash n-*minus*-2 s after the flash n-1. It corresponds to the $Tyr_Z^{\bullet}Q_A^{\bullet-}$-

minus-Tyr_ZQ_A difference. Finally, the green vertical arrow, 300 ms-*minus*-2 s, in Panel B of Fig.1 corresponds to $Tyr_Z^{\bullet}$-*minus*-Tyr_Z difference alone (in the presence of $Tyr_D^{\bullet}$).

The lower ΔI/I amplitude 200 µs after the first flash compared with subsequent flashes was most likely due to centers in which non-heme iron was oxidized prior to flash illumination. Indeed, in these centers, the electron transfer from $Q_A^{\bullet-}$ to Fe^{3+} is complete much before 200 µs [34,35].

The experiment reported in Fig. 1 was repeated for wavelengths from 401 nm to 457 nm. To improve the signal-to-noise ratio, except for the data corresponding to the first flash, the spectra were averaged from the 6th to 10th flashes. Fig. 2 shows, with the same color code, the five spectra corresponding to the five electrochromic responses defined in Panel B of Fig. 1.

The spectrum in red corresponding to the $Q_A^{\bullet-}$-*minus*-Q_A difference in the presence of both $Tyr_Z^{\bullet}$ and $Tyr_D^{\bullet}$ could be questionable. Indeed, it seems more or less similar to the difference spectrum $[P_{D1}P_{D2}]^{\bullet+}Q_A^{\bullet-}$-*minus*-$[P_{D1}P_{D2}]Q_A$ recorded 20 ns after a flash [36], see also [18]. The amplitude of the $[P_{D1}P_{D2}]^{\bullet+}Q_A^{\bullet-}$ spectrum at 432 nm, 20 ns after the flash, with the same setup and in a similar sample, was ~ 0.016 ΔI/I [36], that is ~ 11 times larger than the red spectrum recorded here. The presence of ~ 10% $[P_{D1}P_{D2}]^{\bullet+}$ at 200 µs after the flash could therefore account for the ΔI/I observed here at 432 nm. However, it is difficult to attribute the species at the origin of the slow decay in the 432-446 nm range [36], see however the data at 820 nm [37]. Indeed, what is measured is in fact the decay of the $[P_{D1}P_{D2}]^{\bullet+}Q_A^{\bullet-}$ spectrum, which obligatory also contains the spectral contributions due to the formation of $Q_A^{\bullet-}$, and most likely, these contributions could be at the origin of the phases in the hundreds µs time range, which corresponds to the electron transfer from $Q_A^{\bullet-}$ to Q_B (there is no transfer to $Q_B^{\bullet-}$ due to the presence of PPBQ), *e.g.* [38]. In addition, the red spectrum in Fig. 2 is very similar, both in term of the shape and amplitude, to the electrochromic shift induced by the formation of $Q_A^{\bullet-}$, attributed to a change of the absorption of P_{D1}, in conditions where the presence of P_{680}^{+} can be excluded [22].

The $Q_A^{\bullet-}$-*minus*-Q_A difference spectrum after the first flash, spectrum in orange, shows a shift to the blue of 2 nm compared with the red spectrum, from ~ 434 nm to ~ 432 nm. This means that the presence of the two tyrosyl radicals shifts the $Q_A^{\bullet-}$-*minus*-Q_A difference spectrum to the red compared with the situation with $Tyr_D^{\bullet}$ alone. As explained above, after the first flash there is a mixing between two difference spectra because $Tyr_Z^{\bullet}$ and $Tyr_D^{\bullet}$ are formed in almost equal proportion [23]. This implies that the difference between the first flash and the average of the 6th to 10th flash would be larger if $Tyr_D^{\bullet}Q_A^{\bullet-}$ had been formed alone

after the first flash. It is also worth noting that the $[P_{D1}P_{D2}]^{\bullet+}$ spectrum measured 20 ns after a flash shows a dip at the same wavelength, ~ 432 nm, after the first and subsequent flashes [36]. This is another argument that makes the attribution of the orange and red spectra to $[P_{D1}P_{D2}]^{\bullet+}$ unlikely.

While the pigment whose absorption is modified by the formation of $Q_A^{\bullet-}$ has clearly been identified as P_{D1}, *e.g.* [21,22] and see below, the pigment(s) affected by the formation of $Tyr_Z^{\bullet}$ and $Tyr_D^{\bullet}$ have yet to be identified. This is the subject of the experiments reported below by using mutants PSII and PSII from different species.

Panel A in Fig. 3 shows the ΔI/I recorded at 432 nm in Mn-depleted Tyr_D-less PSII [27], at pH 8.6, illuminated by 10 saturating flashes (spaced 2 s apart) in the presence of the electron acceptor PPBQ. Although there is no Tyr_D in this PSII, it was also dark-adapted for 3 to 4 hours at room temperature before the flash illumination. Panel B in Fig. 3 shows the spectra constructed as described in Panel B of Fig. 1. Due the lack of Tyr_D, $Tyr_Z^{\bullet}$ was formed on the first flash, and the black spectrum recorded 2 s after the first flash is consequently attributed to the $Tyr_Z^{\bullet-}$-*minus*-Tyr_Z spectrum (green spectrum). Two other observations can be made; *i*) the $Q_A^{\bullet-}$-*minus*-Q_A difference spectrum after the first flash, in orange, is identical to the $Q_A^{\bullet-}$-*minus*-Q_A difference spectrum after the following flashes, and *ii*) the trough of this spectrum in the presence of $Tyr_Z^{\bullet}$ alone is at ~ 433 nm that is intermediate between the $Q_A^{\bullet-}$-*minus*-Q_A difference spectrum in the presence of either $Tyr_D^{\bullet}$ alone or both $Tyr_D^{\bullet}$ and $Tyr_Z^{\bullet}$. This experiment shows that in the three situations with either $Tyr_D^{\bullet}$, or $Tyr_Z^{\bullet}$, or $Tyr_D^{\bullet}$ and $Tyr_Z^{\bullet}$, the $Q_A^{\bullet-}$-*minus*-Q_A difference spectrum slightly differs.

In Mn-depleted PSII, and at pH 6.5, both the oxidation of Tyr_Z and Tyr_D are coupled to a proton release into the bulk [39,40]. In [39] it has been proposed that the proton released upon the formation of $Tyr_D^{\bullet}$ was directly released from the protein and not transferred to the neighbouring D2-His198 in contrast to what happens upon the formation of $Tyr_Z^{\bullet}$, in which the proton is transferred to the H-bonded D1-His190. At pH 8.6, a pH value where $Tyr_D^{\bullet}$ is not stable in the dark, nothing is known about the proton release following the oxidation of Tyr_D. Fig. 4 reports an experiment in which, by using the dye thymol blue, the proton release into the bulk has been followed at pH 8.6 after a series of flashes given on dark-adapted Mn-depleted PsbA3-PSII. At 580 nm, an acidification of the medium induces a decrease in the absorption of thymol blue. The sample was illuminated by ten flashes, spaced 2 s apart, and the ΔI/I were measured every 100 ms (the first detector was given 20 μs after the actinic flashes). The black trace corresponds to the raw data. The red curve corresponds to a polynomial curve and the blue trace is the black trace *minus* the polynomial curve. This

procedure has been done to subtract as much as possible the drift in the black trace. Despites the bubbling of the PSII suspension with a pure Argon gas, the drift very likely occurs from the solubilisation of traces of atmospheric CO_2.

The first conclusion that can be drawn from the experiment shown in Fig. 4 is that Tyr_D oxidation is not coupled to a release of proton into the bulk as shown by the absence of a color change of thymol blue after the first flash. This contrasts with what happens when Tyr_Z is oxidized in subsequent flashes where a proton was released with a kinetics not resolved in this experiment. The decay of $Tyr_Z^{\bullet}$ was then coupled to a proton uptake by PSII with a kinetics similar to that one at 432 nm in Fig. 1A. To our knowledge this is the first measurement of the proton release/uptake at pH 8.6 coupled to the oxidation of Tyr_D and then Tyr_Z. The second conclusion we can draw is that both the oxidations of Tyr_Z and Tyr_D have an electrochromic effect on one or more pigments, whereas in the case of Tyr_Z oxidation, the proton is released into the medium and in the case of Tyr_D the proton is not.

In the following, we present some comparisons of the different spectra defined in Panel B of Fig. 1, which have been obtained in Mn-depleted PSII from mutants PSII and from PSII with different pigment compositions namely the D1/H198Q [25], D1/T179H [26], and D2/I178H [28] mutants, and FRL-PSII from *C. thermalis* with 4 Chl-*f* and 1 Chl-*d* [20] and PSII from *A. marina* with 1 Chl-*a* (P_{D1}) and 34 Chl-*d* [29].

Panel A in Fig. 5 shows the $Tyr_Z^{\bullet}Q_A^{\bullet-}$-*minus*-$Tyr_Z^{\bullet}Q_A$ difference spectra in PsbA3-PSII (black spectrum), D1/H198Q-PSII (red spectrum), D1/T179H-PSII (blue spectrum), and FRL-PSII from *C. thermalis* (green spectrum). As expected, the larger main modification was observed in the D1/H198Q mutant in which the axial ligand of P_{D1} has been modified. The trough was shifted to the blue, by ~ 3-4 nm, from 433-434 nm in PsbA3-PSII to 430 nm in the mutant. The $Tyr_Z^{\bullet}Q_A^{\bullet-}$-*minus*-$Tyr_Z^{\bullet}Q_A$ difference spectrum in PsbA3-PSII exhibited a shoulder at 443-444 nm. This shoulder was not shifted in the D1/H198Q-PSII. In contrast, in the FRL-PSII, in which Chl_{D1} is very likely a Chl-*d*, this shoulder was shifted to the red by ~ 3 nm. This shift is accompanied by a narrowing of the spectrum between 434 nm and 440 nm, confirming the shift of a spectral component towards the red. In the D1/T179H mutant, where Chl_{D1} is also affected, the shoulder at 443-444 nm seems also modified, but much less obviously.

Panel B in Fig. 5 shows the $Tyr_Z^{\bullet}Q_A^{\bullet-}$-*minus*-$Tyr_ZQ_A$ difference spectra in PsbA3-PSII (black spectrum), D1/H198Q-PSII (red spectrum), D1/T179H-PSII (blue spectrum), and FRL-PSII from *C. thermalis* (green spectrum). The shape of these spectra suggests that two pigments absorbing around 430 nm have a spectrum shifted by the formation of $Tyr_Z^{\bullet}Q_A^{-}$,

with the absorption of one of the 2 pigments shifted towards the blue and the other towards the red. The effect of the D1/H198Q mutation shows that one of the two pigments is clearly P_{D1}. In a previous study done in O_2 evolving PSII [41], and performed at pH 6.5, we have interpreted a similar spectra upon $Tyr_Z^{\bullet}Q_A^{\bullet-}$ formation as originating from a red shift of the Soret band of P_{D1} and a blue shift of the Soret band of Chl_{D1}. Unfortunately, the signal-to-noise ratio of the current spectra, compared with previous ones in [41], is not good enough to confirm or deny the involvement of Chl_{D1} in the $Tyr_Z^{\bullet}Q_A^{\bullet-}$-*minus*-$Tyr_ZQ_A$ difference spectrum under the conditions used here.

Panel C in Fig. 5 shows the $Tyr_Z^{\bullet}$-*minus*-Tyr_Z difference spectra in PsbA3-PSII (black spectrum), D1/H198Q-PSII (red spectrum), D1/T179H-PSII (blue spectrum), and FRL-PSII from *C. thermalis* (green spectrum). The shape of these spectra also suggests that more than 1 pigment absorbing around 430 nm have a spectrum modified by the formation of $Tyr_Z^{\bullet}$ when compared to Tyr_Z. Surprisingly, the spectrum was not modified in the D1/H198Q mutant. This strongly suggests that P_{D1} has not its absorption shifted by the formation of $Tyr_Z^{\bullet}$. At the same time, this confirms that pigments other than P_{D1} undergo electrochromic shifts in the presence of $Tyr_Z^{\bullet}$. Unfortunately, despite averaging a large number of spectra, the signal-to-noise ratio of the spectra remained too modest to clearly identify these pigments. However, given the spectral range in which the band shifts are observed, and the lack of effect in the mutants studied, it seems possible that a carotenoid or pigment other than P_{D1}, Chl_{D1}, Chl_{D2} may be involved.

Panel D in Fig. 5 shows the $Tyr_D^{\bullet}$-*minus*-Tyr_D difference spectra in PsbA3-PSII (black spectrum), D1/H198Q-PSII (red spectrum), D1/T179H-PSII (blue spectrum), D2/I178H (orange spectrum) [28], and FRL-PSII from *C. thermalis* (green spectrum). These spectra significantly differ from the $Tyr_Z^{\bullet}$-*minus*-Tyr_Z difference spectra. For example, the $Tyr_D^{\bullet}$-*minus*-Tyr_D difference spectra seem to concern only one pigment with a shift from ~ 430 nm in the presence of Tyr_D to ~ 446 nm in the presence of $Tyr_D^{\bullet}$. From the lack of a change in the difference spectrum in the mutants tested, it seems that neither P_{D1}, nor Chl_{D1} nor Chl_{D2} seems to be involved.

The situation in the FRL-PSII (green spectrum) needs to be commented a bit more. Indeed, we observed that in the dark-adapted FRL-PSII the proportion of centers with a reduced Tyr_D is highly variable with virtually no reduction in some cases, as confirmed by the amplitude of the $Tyr_D^{\bullet}$ signal in EPR before and after an illumination (not shown). This suggests a major difference with other PSII. The reason for this has not been investigated further, but it means that the $Tyr_D^{\bullet}$-*minus*-Tyr_D difference spectrum may be contaminated by

a contribution from the $Tyr_Z^{\bullet}$-*minus*-Tyr_Z difference. That said, it seems that the positive part of the spectrum in the presence of $Tyr_D^{\bullet}$ seems to have shifted to ~ 449 nm in FRL-PSII instead of ~ 446 nm in the other samples. Nevertheless, the fact that the spectrum of this pigment has a maximum at 430 nm in the presence of Tyr_D, as in other PSII, indicates that the pigment involved does not have a modified spectrum, but that it is the electrochromic effect that is different. This difference is probably due to a modified electrostatic environment in PSII-FRL, as already mentioned, and possibly at the origin of the different stability of $Tyr_D^{\bullet}$.

One pigment not investigated until now in this report is P_{D2}. To do it we have used PSII from *Synechocystis* 6803 in which the D2/H197A mutant has been constructed [30]. The results are shown in Fig. 6 for the 4 difference spectra. Surprisingly, even the $Tyr_D^{\bullet}$-*minus*-Tyr_D difference spectrum remained unaffected by the D2/H197A mutation.

The lack of significant effects except with the P_{D1} mutant, D1/H198Q, in the two cases corresponding to the $Tyr_Z^{\bullet}Q_A^{\bullet-}$-*minus*-$Tyr_ZQ_A$ and $Tyr_Z^{\bullet}Q_A^{\bullet-}$-*minus*-$Tyr_Z^{\bullet}Q_A$ difference spectra suggests that, as said above, either pigments other than P_{D2}, Ch_{D1} and Chl_{D2} are affected or that the spectral changes are too weak taking into account the signal-to-noise ratio of the experiments. One way of confirming this hypothesis is to look at what happens in the PSII of *A. marina* with 34 Chl-*d* and one Chl-*a*.

It was reported that the $P_{680}^{\bullet+}Q_A^{\bullet-}$-*minus*-$P_{680}Q_A$ difference spectrum at 77 K was identical to that in *T. elongatus* [31], which led the authors to confirm that P_{D1} was the Chl-*a*. Here, we looked at the $Tyr_D^{\bullet}$-*minus*-Tyr_D and $Tyr_Z^{\bullet}$-*minus*-Tyr_Z difference spectra. In *A marina*, unlike in *T. vestitus*, $Tyr_D^{\bullet}$ is not stable in the dark at pH 6.5, which led us to make the difference spectra at pH 6.5. Of course, it would have been preferable to record them at pH 8.6, but, unfortunately, for a number of reasons beyond our control, we could not do that.

Fig. 7 shows the $Tyr_D^{\bullet}$-*minus*-Tyr_D (Panel A) and $Tyr_Z^{\bullet}$-*minus*-Tyr_Z (Panel B) difference spectra, at pH 6.5, in FRL-PSII from *C. thermalis* (black spectra), and in PSII from *A. marina* (red spectra). As expected, $Tyr_D^{\bullet}$ appeared stable at pH 6.5 in *C. thermalis* with a $Tyr_D^{\bullet}$-*minus*-Tyr_D difference spectrum completely flat in this PSII at this pH. In contrast, in *A. marina* there was a large $Tyr_D^{\bullet}$-*minus*-Tyr_D difference spectrum. One species whose spectrum is modified by the oxidation of Tyr_D absorbed at ~ 455 nm. This supports the hypothesis that this species is a Chl-*d*. It is tempting to propose that this Chl-*d* has an absorption shifted to ~ 470 nm in the presence of $Tyr_D^{\bullet}$. However, the origin of the positive feature at ~ 422 nm is less clear. For the $Tyr_Z^{\bullet}$-*minus*-Tyr_Z difference spectra, the situation is even less clear-cut. While the possible presence of 2 spectral shifts in *A. marina* may be due

to the doubling of the Soret band on either side of the Soret band for Chl-*a*. The differences between pH 6.5 and pH 8.6 in the case of *C. thermalis* remain to be understood.

Panel B in Fig. 1 shows that between 10 ms and 500 ms a change in the ΔI/I occurred in the opposite direction when compared to the decay of $Tyr_Z^{\bullet}$. Panel A in Fig. 8 shows an average of the ΔI/I from the 6th to 10th flash in PsbA3-PSII from *T. vestitus* (black points), D1/H198Q-PSII (red points), and FRL-PSII from *C. thermalis* (green points). Panel B in Fig. 8 shows the spectra in the 3 PSII. The 3 spectra are identical to the difference spectra $Tyr_Z^{\bullet}Q_A^{\bullet-}$-*minus*-$Tyr_ZQ_A$ head-to-tail. This suggests that the electrostatic environment resulting from the formation of $Tyr_Z^{\bullet}Q_A^{\bullet-}$ occurs with a kinetics slower than the formation of the state. The different kinetics in Panel A of Fig. 8 could be another manifestation of a different rearrangement of the electrostatic environment in the species studied here

Conclusion

The effects of $Tyr_D^{\bullet}$, $Tyr_Z^{\bullet}$, and $Q_A^{\bullet-}$ radical formation on the absorption spectrum in the Soret region were studied in Mn-depleted Photosystem II at pH 8.6. Flash-induced difference spectra were recorded in several PSII samples from *i*) *Thermosynechococcus vestitus* (formerly *T. elongatus*), *ii*) *Synechocystis* sp. PCC 6803, *iii*) *Chroococcidiopsis thermalis* PCC7203 grown under far-red light, and *iv*) *Acaryochloris marina*. While P_{D1} is clearly the species whose spectrum is blue shifted by ~ 3 nm in the presence of $Q_A^{\bullet-}$, from the spectra recorded in these different samples P_{D1}, P_{D2}, Chl_{D1}, Phe_{D1}, and Chl_{D2} seems not the species whose the absorption spectrum is modified by the formation of $Tyr_D^{\bullet}$ and $Tyr_Z^{\bullet}$. The conclusion for Phe_{D1} comes from the similarity of the $Tyr_Z^{\bullet}$-*minus*-Tyr_Z difference spectrum in PsbA3-PSII with E130 and PsbA1/Y160F-PSII with Q-130, *e.g.* [42]. It is therefore proposed that other pigments are involved as antenna Chl and/or Car near the reaction center. Additionally, it is shown that, *i*) there is no proton release into the bulk upon the oxidation of Tyr_D at pH 8.6, and *ii*) the rearrangement of the electrostatic environment of the pigments involved in the light-induced different spectra in the samples studied upon the formation $Tyr_D^{\bullet}$, $Tyr_Z^{\bullet}$, and $Q_A^{\bullet-}$ likely occur differently on a kinetic and structural point of views.

Legends

Figure 1:

Panel A shows the ΔI/I changes recorded at 432 nm in Mn-depleted PsbA3-PSII from *T. vestitus* at pH 8.6. The sample was dark adapted for 3 to 4 hours to allow Tyr_D to be almost fully reduced. After the dark adaptation 100 µM of PPBQ, dissolved in dimethyl sulfoxide, were added. Flash illumination was done with 10 saturating flashes (spaced 2 s apart). The first weak detector laser flash was given 200 µs after each of the saturating actinic laser flashes. The second detector flash was given 10 ms after each of the actinic flashes. Then, 20 detector flashes (spaced 100 ms apart) were given after each of the 10 actinic flashes. The OD of the sample was 1.75 at 673 nm (~ 25 µg Chl/ml). The pathlength of the cuvette was 2.5 mm.

Panel B shows the same data as in Panel A with an expanded time-scale for the first 4 actinic flashes. The vertical black arrow, 2 s after the first flash, corresponds to the Δ(ΔI/I) mainly originating from the formation of $Tyr_D^{\bullet}$ alone since $Q_A^{\bullet-}$ and $Tyr_Z^{\bullet}$ (formed in centers in which Tyr_D was not in the reduced state) are no longer present 2 s after the flash. After the 4th flash, when $Tyr_D^{\bullet}$ has been formed in the great majority of centers, the flash illumination induced the formation of the $Tyr_Z^{\bullet}Q_A^{\bullet-}$ state. The vertical red arrow shows the Δ(ΔI/I) between 200 µs and 10 ms and corresponds to the $Tyr_Z^{\bullet}Q_A^{\bullet-}$-*minus*-$Tyr_Z^{\bullet}Q_A$ difference. The vertical violet arrow shows the Δ(ΔI/I) between 200 µs and 2 s and corresponds to the $Tyr_Z^{\bullet}Q_A^{\bullet-}$-*minus*-$Tyr_ZQ_A$ difference. The vertical green arrow shows the Δ(ΔI/I) between 400 ms and 2 s and corresponds to the $Tyr_Z^{\bullet}$-*minus*-Tyr_Z difference. The vertical orange arrow shows the Δ(ΔI/I) between 200 µs and 10 ms after the 1st actinic flash and corresponds to the $Q_A^{\bullet-}$-*minus*-Q_A difference (in the presence of $Tyr_D^{\bullet}$). The Δ(ΔI/I) between 10 ms and 400 ms will be analyzed in Fig. 8.

Figure 2:

The experiment done at 432 nm with PsbA3-PSII of *T. vestitus* and reported in Panel A of Fig. 1 was repeated for wavelengths between 401 nm and 457 nm and the different Δ(ΔI/I) defined in Panel B of Fig. 1 have been plotted with the color code defined in Panel B of Fig. 1. Except for the spectra corresponding to the first flash, the Δ(ΔI/I) were averaged from the 6th to 10th flash.

Figure 3:

Panel A shows the ΔI/I changes recorded at 432 nm in Mn-depleted Tyr_D-less PSII from *T. vestitus* at pH 8.6 with the same protocol as described in Panel A of Fig. 1.

Panel B; the ΔI/I were measured as in Panel A for wavelengths between 401 nm and 457 nm and have been plotted with the color code defined in Panel B of Fig. 1. Except for the spectra corresponding to the first flash, the Δ(ΔI/I) were averaged from the 6th to 10th flash.

Figure 4:

ΔI/I changes recorded at 580 nm in the presence of thymol blue (black data points) with the dark-adapted Tyr_D-less PSII from *T. vestitus* at pH 8.6. The first detector flash was given 20 µs after each actinic flash. Then, 20 detector flashes (spaced 100 ms apart) were given after each of the 10 actinic flashes. The continuous red curve corresponds to a polynomial function of the second degree. The blue trace is the black trace *minus* the red curve. This procedure was done to subtract as much as possible the drift in the black trace.

Figure 5:

Panel A, spectra of the $Tyr_Z^{\bullet}Q_A^{\bullet-}$-*minus*-$Tyr_Z^{\bullet}Q_A$ difference in various PSII samples. Same conditions as in Panels A and B in Fig. 1.

Panel B, spectra of the $Tyr_Z^{\bullet}Q_A^{\bullet-}$-*minus*-$Tyr_ZQ_A$ difference in various PSII samples. Same conditions as in Panels A and B in Fig. 1.

Panel C, spectra of the $Tyr_Z^{\bullet}$-*minus*-Tyr_Z difference in various PSII samples. Same conditions as in Panels A and B in Fig. 1.

Panel D, spectra of the $Tyr_D^{\bullet}$-*minus*-Tyr_D difference in various PSII samples. Same conditions as in Panels A and B in Fig. 1.

All the spectra were normalized to -1 for the amplitude of the trough.

Figure 6:

Panel A, spectra of the $Tyr_Z^{\bullet}Q_A^{\bullet-}$-*minus*-$Tyr_Z^{\bullet}Q_A$ difference in wild type *Synechocystis* 6803 (black spectrum) and in the D2/H197A mutant (green spectrum). Same conditions as in Panels A and B in Fig. 1.

Panel B, spectra of the $Tyr_Z^{\bullet}Q_A^{\bullet-}$-*minus*-$Tyr_ZQ_A$ difference in wild type *Synechocystis* 6803 (black spectrum) and in the D2/H197A mutant (green spectrum). Same conditions as in Panels A and B in Fig. 1.

Panel C, spectra of the $Tyr_D^{\bullet}$-*minus*-Tyr_D difference in wild type *Synechocystis* 6803 (black spectrum) and in the D2/H197A mutant (green spectrum). Same conditions as in Panels A and B in Fig. 1.

Panel D, spectra of the $Tyr_Z^{\bullet}$-*minus*-Tyr_Z difference in wild type *Synechocystis* 6803 (black spectrum) and in the D2/H197A mutant (green spectrum). Same conditions as in Panels A and B in Fig. 1.

All the spectra were normalized to -1 for the amplitude of the trough.

Figure 7:

Panel A, spectra of the $Tyr_D^{\bullet}$-*minus*-Tyr_D difference at pH 6.5 in *C. thermalis* (black spectrum) and in PSII from *A. marina* (red spectrum). Other conditions same as in Panels A and B in Fig. 1.

Panel B, spectra of the $Tyr_Z^{\bullet}$-*minus*-Tyr_Z difference at pH 6.5 in FRL-PSII from *C thermalis* (black spectrum) and in PSII from *A. marina* (red spectrum). Other conditions same as in Panels A and B in Fig. 1. The ΔI/I were averaged from the 6th to 10th flash.

Figure 8:

Panel A, ΔI/I recorded at 432 nm and at pH 8.6 in Mn-depleted PSII from *C. thermalis* (green data points), from *T. vestitus* (black data points), and from the D1/H198Q mutant in *T. vestitus* (red data points). The ΔI/I were averaged from the 6th to 10th flash. The first point corresponds to the detector given 10 ms after the actinic flash.

Panel B shows the wavelength dependence of the maximum amplitude of the kinetics in Panel A that are at 300 ms for the PsbA3-PSII from *T. vestitus*, at 100 ms for the FRL-PSII from *C. thermalis*, and 500 ms for the D1/H198Q PSII from *T. vestitus*.

References

[1] Y. Umena, K. Kawakami, J.-R. Shen, N. Kamiya, Crystal structure of oxygen evolving Photosystem II at a resolution of 1.9 angstrom, Nature 473 (2011) 55–60, https://doi.org/10.1038/nature09913

[2] H. Ago, H. Adachi, Y. Umena, T. Tashiro, K. Kawakami, N. Kamiya, L.R. Tian, G.Y. Han, T.Y. Kuang, Z.Y. Liu, F.J. Wang, H.F. Zou, I. Enami, M. Miyano, J.-R. Shen, Novel features of eukaryotic photosystem II revealed by its crystal structure analysis from a red alga, J. Biol. Chem. 291 (2016) 5676–5687, https://doi.org/10.1074/jbc.M115.711689

[3] C.J. Gisriel, J. Wang, J. Liu, D.A. Flesher, K.M. Reiss, H.-L. Huang, K.R. Yang, W.H. Armstrong, M.R. Gunner, V.S. Batista, R.J. Debus, G.W. Brudvig, High resolution cryo-electron microscopy structure of photosystem II from the mesophilic cyanobacterium, *Synechocystis* sp. PCC 6803, Proc. Natl. Acad. Sci. U. S. A. 119 (2022), e2116765118, https://doi.org/10.1073/pnas.2116765118

[5] A.R. Holzwarth, M.G. Müller, M. Reus, M. Nowaczyk, J. Sander, M. Rögner, Kinetics and mechanism of electron transfer in intact Photosystem II and in the isolated reaction center: pheophytin is the primary electron acceptor, Proc. Natl. Acad. Sci. U. S. A. 103 (2006) 6895–6900, https://doi.org/10.1073/pnas.0505371103

[6] F. Muh, M. Plockinger, T. Renger, Electrostatic asymmetry in the reaction center of Photosystem II, J. Phys. Chem. Lett. 8 (2017) 850–858, https://doi.org/10.1021/acs.jpclett.6b02823

[7] A. Sirohiwal, D.A. Pantazis, Reaction center excitation in Photosystem II: From multiscale modeling to functional principles, Acc. Chem. Res. (2023) 2921−2932. https://doi.org/10.1021/acs.accounts.3c00392

[8] D.J. Vinyard, G.M. Ananyev, G.C. Dismukes, Photosystem II: the reaction center of oxygenic photosynthesis, Annu. Rev. Biochem. 82 (2013) 577–606. https://10.1146/annurev-biochem-070511-100425

[9] D. Shevela J.F. Kern G. Govindjee J. Messinger , Solar energy conversion by photosystem II: principles and structures, Photosynth. Res. 156 (2023) 279–307. https://doi.org/10.1007/s11120-022-00991-y

[10] W. Lubitz D.A. Pantazis N. Cox , Water oxidation in oxygenic photosynthesis studied by magnetic resonance techniques, FEBS Lett. 597 (2023) 6–29. https://doi.org/10.1002/1873-3468.14543

[11] N. Oliver, A.P. Avramov, D.J. Nürnberg, H. Dau, R.L. Burnap, From manganese oxidation to water oxidation: assembly and evolution of the water-splitting complex in photosystem II, Photosynth. Res. 152 (2022) 107–133, https://doi.org/10.1007/s11120-022-00912-z

[12] T. Oliver, T.D. Kim, J.P. Trinugroho, V. Cord´on-Preciado, N. Wijayatilake, A. Bhatia, A.W. Rutherford, T. Cardona, The evolution and evolvability of photosystem II, Annu. Rev. Plant Biol. 74 (2023) 24.1–24.33, https://doi.org/10.1146/annurev-arplant-070522-062509

[13] P. Joliot, Period-four oscillations of the flash-induced oxygen formation in photosynthesis, Photosynth. Res. 76 (2003) 65–72. https://doi.org/10.1023/A:1024946610564

[14] B. Kok, B. Forbush, M. McGloin, Cooperation of charges in photosynthetic O_2 evolution–I. A linear four step mechanism, Photochem. Photobiol. 11 (1970) 457–475, https://doi.org/10.1111/j.1751-1097.1970.tb06017.x

[15] E.J. Bylina, C. Kirmaier, L. McDowell, D. Holten, D.C. Youvan, Influence of an amino-acid residue on the optical properties and electron transfer dynamics of a photosynthetic reaction center complex, Nature 336 (1988) 182–184. https://doi.org/10.1038/336182a0

[16] D.H. Stewart, P.J. Nixon, B.A. Diner, G.W. Brudvig, Assignment of the Qy absorbance bands of photosystem II chromophores by low-temperature optical spectroscopy of wild-type and mutant reaction centres, Biochemistry 39 (2000) 14583–14594. https://doi.org/10.1021/bi001246j

[17] L.B. Giorgi, P.J. Nixon, S.A.P. Merry, D.M. Joseph, J.R. Durrant, J.D. Rivas, J. Barber, G. Porter, D.R. Klug, Comparison of primary charge separation in the photosystem II reaction center complex isolated from wild-type and D1–130 mutants of the cyanobacterium Synechocystis PCC 6803, J. Biol. Chem. 271 (1996) 2093–2101. https://doi.org/10.1074/jbc.271.4.2093

[18] B.A. Diner, E. Schlodder, P.J. Nixon, W.J. Coleman, F. Rappaport, J. Lavergne, W.F. J. Vermaas, D.A. Chisholm, Site-directed mutations at D1-His198 and D2-His197 of photosystem II in *Synechocystis* PCC 6803: sites of primary charge separation and cation and triplet stabilization, Biochemistry 24 (2001) 9265–9281. https://doi.org/10.1021/bi010121r

[19] E. Schlodder, W.J. Coleman, P.J. Nixon, R.O. Cohen, T. Renger, B.A. Diner, Site directed mutations at D1-His198 and D1-Thr179 of photosystem II in *Synechocystis* sp. PCC 6803: deciphering the spectral properties of the PSII reaction centre, Philos. Trans. R. Soc. B 363 (2008) 1197−1202. https://doi.org/10.1098/rstb.2007.2215

[20] D.J. Nürnberg, J. Morton, S. Santabarbara, A. Telfer, P. Joliot, L.A. Antonaru, A. H. Ruban, T. Cardona, E. Krausz, A. Boussac, A. Fantuzzi, A.W. Rutherford, Photochemistry

beyond the red-limit in the chlorophyll f-containing photosystems, Science 360 (2018) 1210–1213. https://doi.org/10.1126/science.aar8313

[21] F. Rappaport, M. Blanchard-Desce, J. Lavergne, Kinetics of electron-transfer and electrochromic change during the redox transitions of the photosynthetic oxygen evolving complex, Biochim. Biophys. Acta 1184 (1994) 178–192. https://doi.org/10.1016/0005-2728(94)90222-4

[22] F. Rappaport, J. Lavergne, Proton release during successive oxidation steps of the photosynthetic water oxidation process: stoichiometries and pH dependence, Biochemistry 30 (1991) 10004–10012. https://doi.org/10.1021/bi00105a027

[23] P. Faller, R.J. Debus, K. Brettel, M. Sugiura, A.W. Rutherford, A. Boussac, Rapid formation of the stable tyrosyl radical in photosystem II, Proc Natl Acad Sci USA 98 (2001)14368–14373. https://doi.org/10.1073/pnas.251382598

[24] M. Sugiura, A. Boussac, T. Noguchi, F. Rappaport, Influence of Histidine-198 of the D1 subunit on the properties of the primary electron donor, P680, of photosystem II in *Thermosynechococcus elongatus*, Biochim. Biophys. Acta 1777 (2008) 331–342, https://doi.org/10.1016/j.bbabio.2008.01.007

[25] M. Sugiura, Y. Osaki, F. Rappaport, A. Boussac, Corrigendum to “Influence of Histidine-198 of the D1 subunit on the properties of the primary electron donor, P680, of Photosystem II in *Thermosynechococcus elongatus*”. Biochim. Biophys. Acta 1857 (2016)1943–1948. https://doi.org/10.1016/j.bbabio.2016.09.012

[26] Y. Takegawa, M. Nakamura, S. Nakamura, T. Noguchi, J. Sellés, A.W. Rutherford, A. Boussac, M. Sugiura, New insights on Chl_{D1} function in photosystem II from site-directed mutants of D1/T179 in *Thermosynechococcus elongatus*, Biochim. Biophys. Acta 1860 (2019) 297–309. https://doi.org/10.1016/j.bbabio.2019.01.008

[27] M. Sugiura, F. Rappaport, K. Brettel, T. Noguchi, A.W. Rutherford, A. Boussac , Site-directed mutagenesis of the *Thermosynechococcus elongatus* photosystem II: the O_2-evolving enzyme lacking the redox-active tyrosine D, Biochemistry 43 (2004) 13549–13563. https://doi.org/10.1021/bi048732h

[28] M. Sugiura, M. Kimura, N. Shimamoto, Y. Takegawa, M. Nakamura, K. Koyama, J. Sellés, A. Boussac, A.W. Rutherford, Tuning of the Chl_{D1} and Chl_{D2} properties in photosystem II by site-directed mutagenesis of neighbouring amino acids, Biochim. Biophys. Acta 1865 (2024) 149013. https://doi.org/10.1016/j.bbabio.2023.149013

[29] S. Viola, W. Roseby, S. Santabarabara, D. Nürnberg, R. Assunção, H. Dau, J. Sellés, A. Boussac, A. Fantuzzi, A.W. Rutherford, Impact of energy limitations on function and

resilience in long-wavelength Photosystem II, eLife 11 (2022) e79890. https://doi.org/10.1101/2022.04.05.486971

[30] T. Hayase, Y. Shimada, T. Mitomi, R. Nagao, T. Noguchi, Triplet delocalization over the reaction center chlorophylls in Photosystem II. J Phys Chem 127 (2023) 1758–1770. https://doi.org/10.1021/acs.jpcb.3c00139

[31] T. Renger, E. Schlodder, The primary electron donor of photosystem II of the cyanobacterium *Acaryochloris marina* is a chlorophyll d and the water oxidation is driven by a chlorophyll a/chlorophyll d heterodimer, J. Phys. Chem. B 112 (2008)7351–7354. https://doi.org/10.1021/jp801900e

[32] D. Béal, F. Rappaport, P. Joliot, A new high-sensitivity 10-ns time-resolution spectrophotometric technique adapted to in vivo analysis of the photosynthetic apparatus, Rev. Sci. Instrum. 70 (1999) 202–207. https://doi.org/10.1063/1.1149566

[33] M. Sugiura, T. Taniguchi, N. Tango, M. Nakamura, J. Sellés, A. Boussac, Probing the role of arginine 323 of the D1 protein in photosystem II function, Physiol. Plant. 171 (2021) 183–199. https://doi.org/10.1111/ppl.13115

[34] B.A. Diner, V. Petrouleas, Q400, the non-heme iron of the Photosystem-II iron-quinone complex – a spectroscopic proble of quinone and inhibitor binding to the reaction center, Biochim. Biophys. Acta 895 (1987) 107–125. https://doi.org/10.1016/S0304-4173(87)80010-1

[35] A. Boussac, M. Sugiura, F. Rappaport, Probing the quinone binding site of photosystem II from Thermosynechococcus elongatus containing either PsbA1 or PsbA3 as the D1 protein through the binding characteristics of herbicides, Biochim. Biophys. Acta 1807 (2010) 119–129, https://doi.org/10.1016/j.bbabio.2010.10.004

[36] A. Boussac, M. Sugiura, M. Nakamura, R. Nagao, T. Noguchi, S. Viola, A. W. Rutherford, J. Sellés, Photosynth. Res. (2023). https://doi.org/10.1007/s11120-023-01049-3

[37] H. Conjeaud, P. Mathis, The effect of pH on the reduction kinetics of P-680 in tris-treated chloroplasts, Biochim. Biophys. Acta 590 (1980) 353–359. https://doi.org/10.1016/0005-2728(80)90206-6

[38] R. de Wijn, H.J. van Gorkom, Kinetics of electron transfer from Q_A to Q_B in Photosystem II, Biochemistry 40 (2001) 11912–1192210. https://doi.org/1021/bi010852r

[39] R. Hienerwadel, S. Gourion-Arsiquaud, M. Ballottari, R. Bassi, B.A. Diner, C. Berthomieu, Formate binding near the redox-active TyrosineD in Photosystem II:

consequences on the properties of Tyr_D, Photosynth. Res. 84 (2005) 139–144. https://doi.org/10.1007/s11120-005-0637-x

[40] S. Nakamura, T. Noguchi, Infrared detection of a proton released from tyrosine Y_D to the bulk upon its photo-oxidation in Photosystem II, Biochemistry 54 (2015) 5045–5053. https://doi.org/10.1021/acs.biochem.5b00568

[41] A. Boussac, J. Sellés, M. Sugiura, What can we still learn from the electrochromic band-shifts in photosystem II? Biochim. Biophys. Acta 2020 (1861) 148176, https://doi.org/10.1016/j.bbabio.2020.148176.

[42] M. Sugiura, C. Azami, K. Koyama, A.W. Rutherford, F. Rappaport, A. Boussac, Modification of the pheophytin redox potential in *Thermosynechococcus elongatus* Photosystem II with PsbA3 as D1, Biochim. Biophys. Acta 1837 (2014) 139–148. https://doi.org/10.1016/j.bbabio.2013.09.009

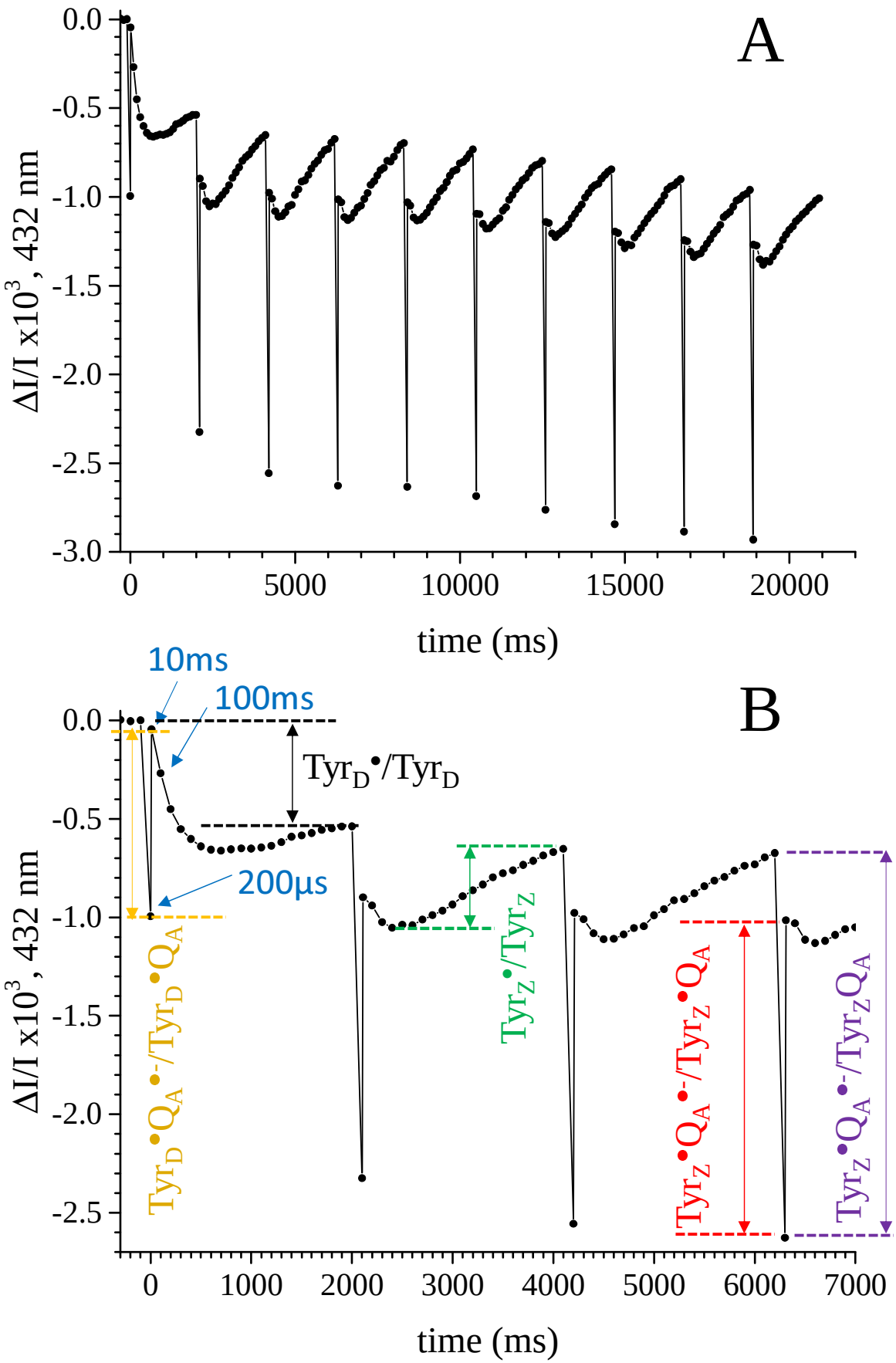
A
0.0
-0.5
-1.0
-1.5
-2.0
-2.5
-3.0
ΔI/I x10^3, 432 nm
0
5000
10000
15000
20000
time (ms)
B
10ms
100ms
200µs
Tyr_D•/Tyr_D
Tyr_D•Q_A•-/Tyr_D•Q_A
Tyr_Z•/Tyr_Z
Tyr_Z•Q_A•-/Tyr_Z•Q_A
Tyr_Z•Q_A•-/$Tyr_Z$$Q_A$
0.0
-0.5
-1.0
-1.5
-2.0
-2.5
ΔI/I x10^3, 432 nm
0
1000
2000
3000
4000
5000
6000
7000
time (ms)

Fig. 1

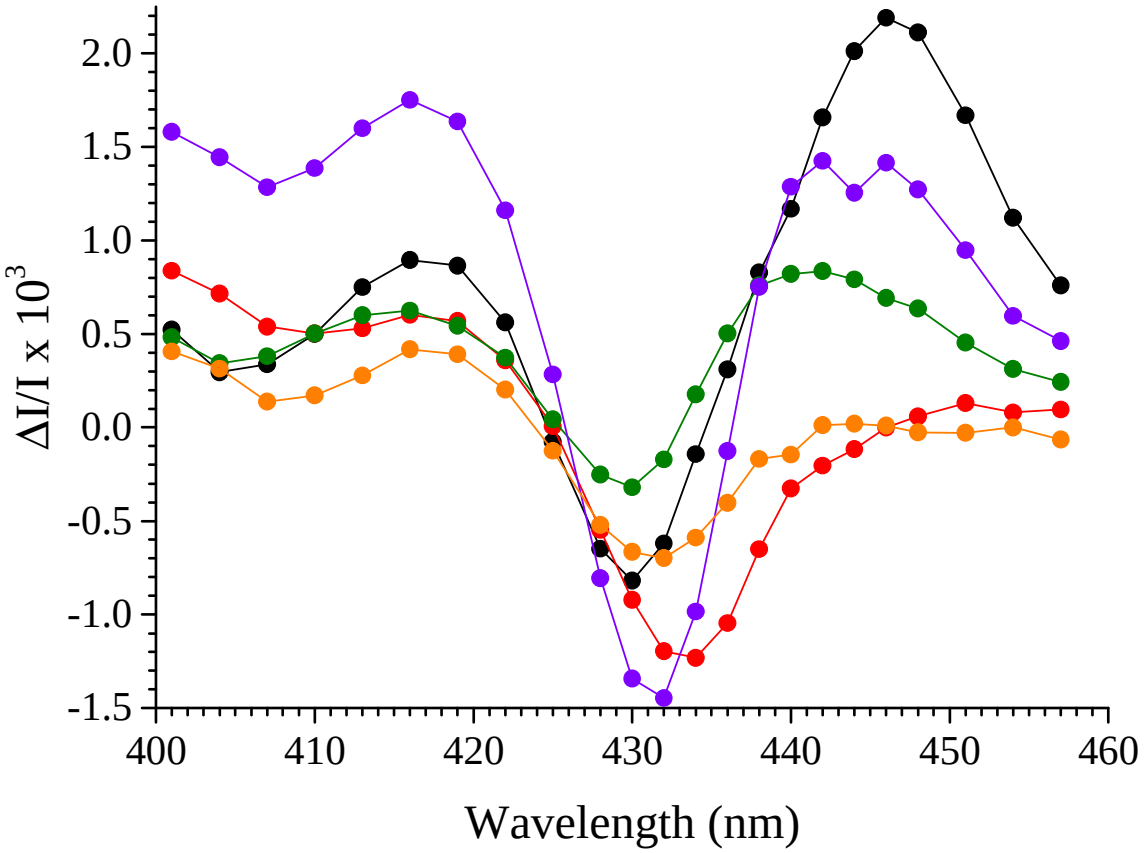
2.0
1.5
1.0
0.5
0.0
-0.5
-1.0
-1.5
ΔI/I x 10^3
400
410
420
430
440
450
460
Wavelength (nm)

Fig. 2

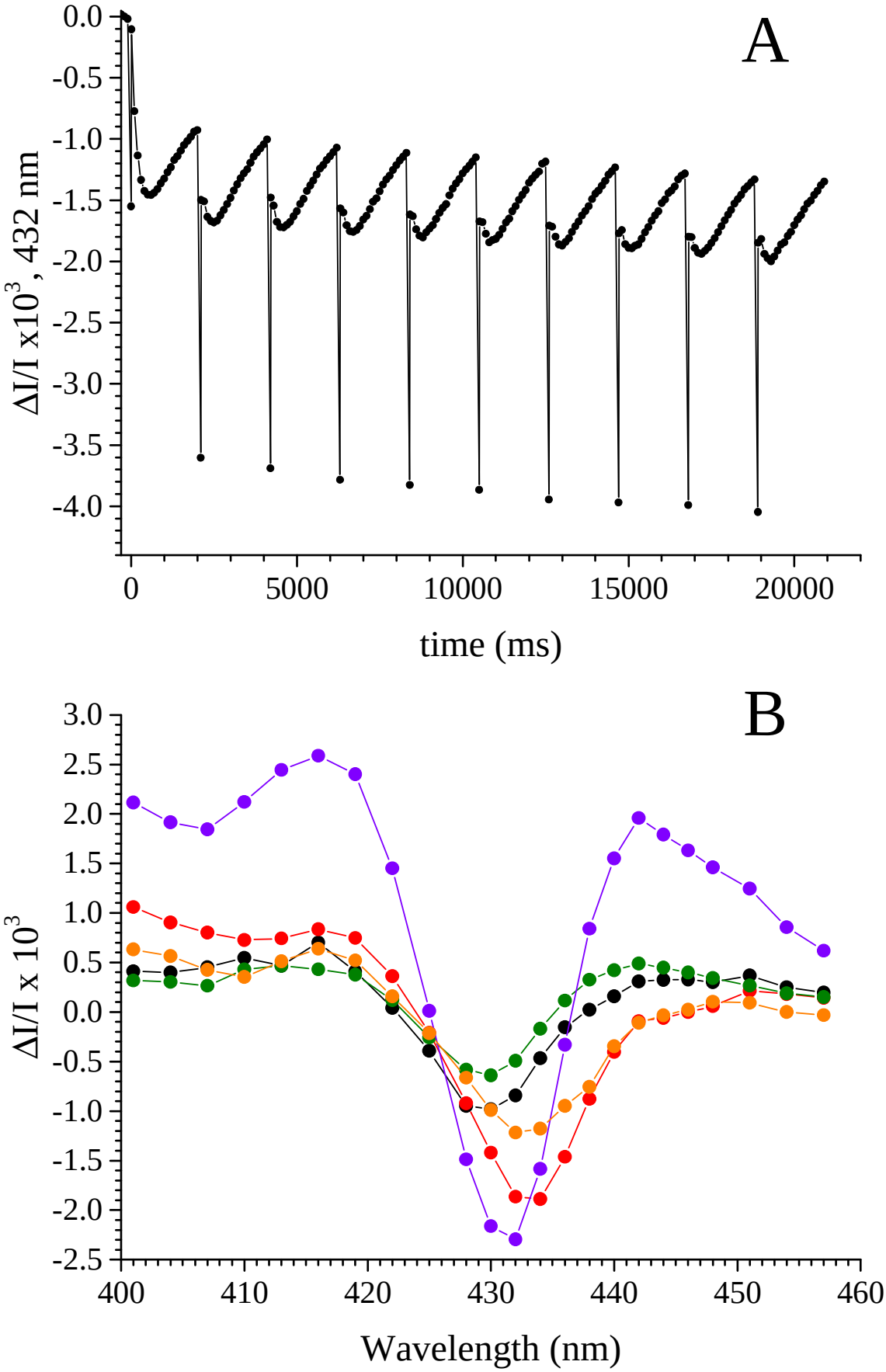
A
0.0
-0.5
-1.0
-1.5
-2.0
-2.5
-3.0
-3.5
-4.0
ΔI/I x10^3, 432 nm
0
5000
10000
15000
20000
time (ms)
B
3.0
2.5
2.0
1.5
1.0
0.5
0.0
-0.5
-1.0
-1.5
-2.0
-2.5
ΔI/I x 10^3
400
410
420
430
440
450
460
Wavelength (nm)

Fig. 3

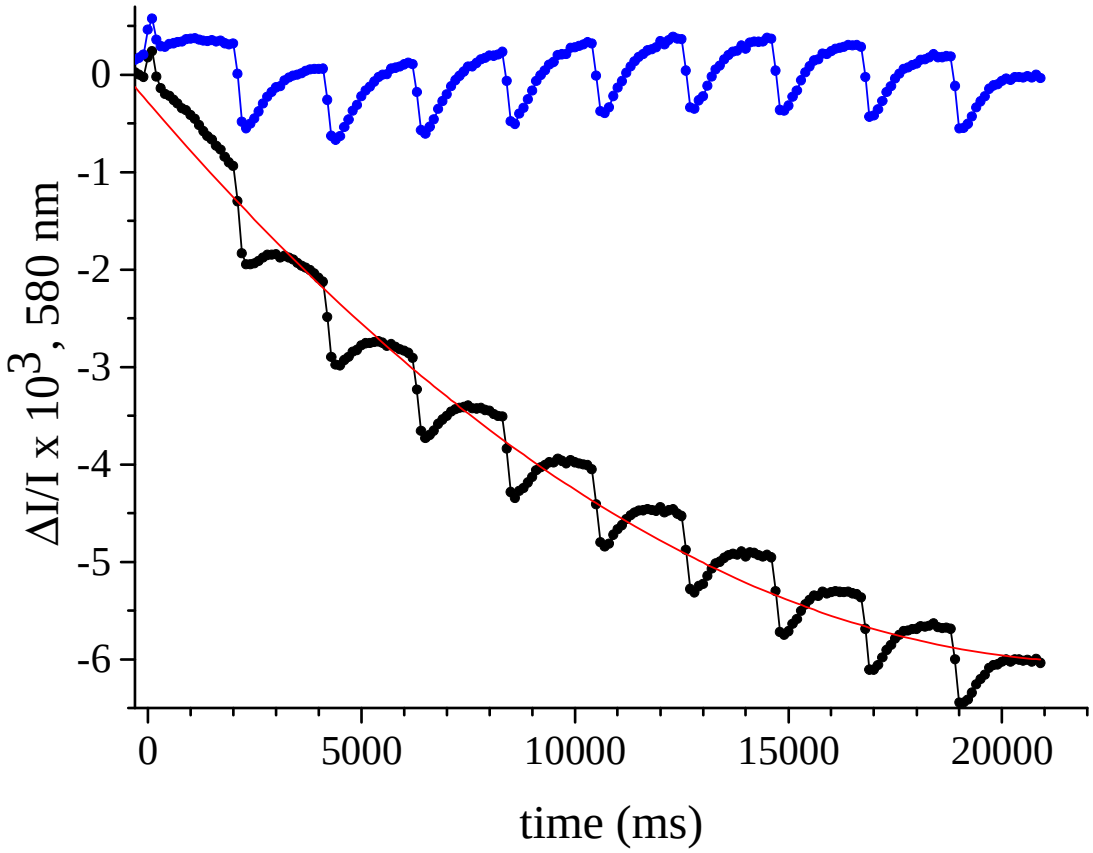

Fig. 4

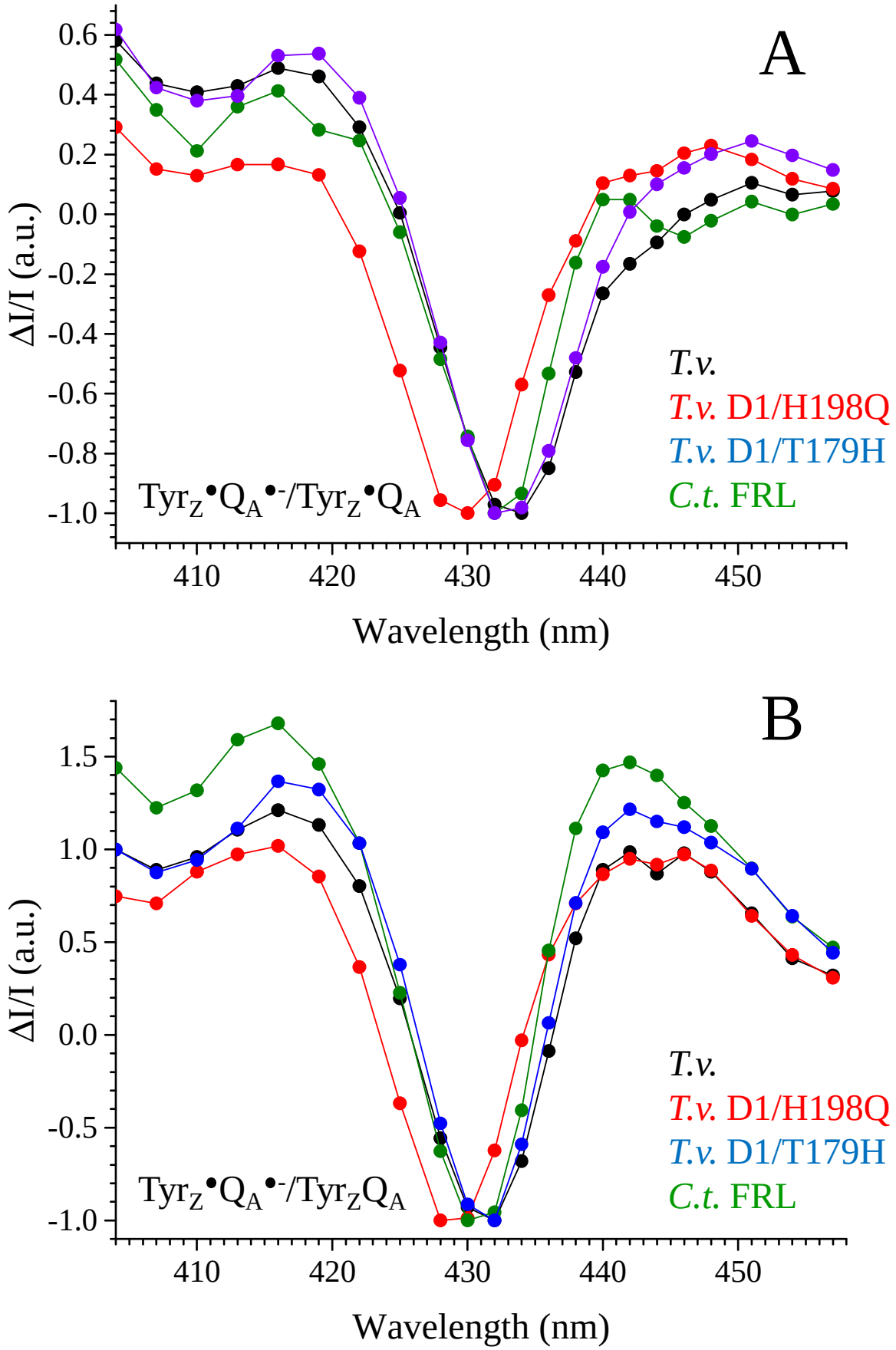
A
0.6
0.4
0.2
0.0
-0.2
-0.4
-0.6
-0.8
-1.0
ΔI/I (a.u.)
410
420
430
440
450
Wavelength (nm)
Tyr$_Z$•Q$_A$•$^-$/Tyr$_Z$•Q$_A$
T.v.
T.v. D1/H198Q
T.v. D1/T179H
C.t. FRL
B
1.5
1.0
0.5
0.0
-0.5
-1.0
ΔI/I (a.u.)
410
420
430
440
450
Wavelength (nm)
Tyr$_Z$•Q$_A$•$^-$/Tyr$_Z$Q$_A$
T.v.
T.v. D1/H198Q
T.v. D1/T179H
C.t. FRL

Fig. 5

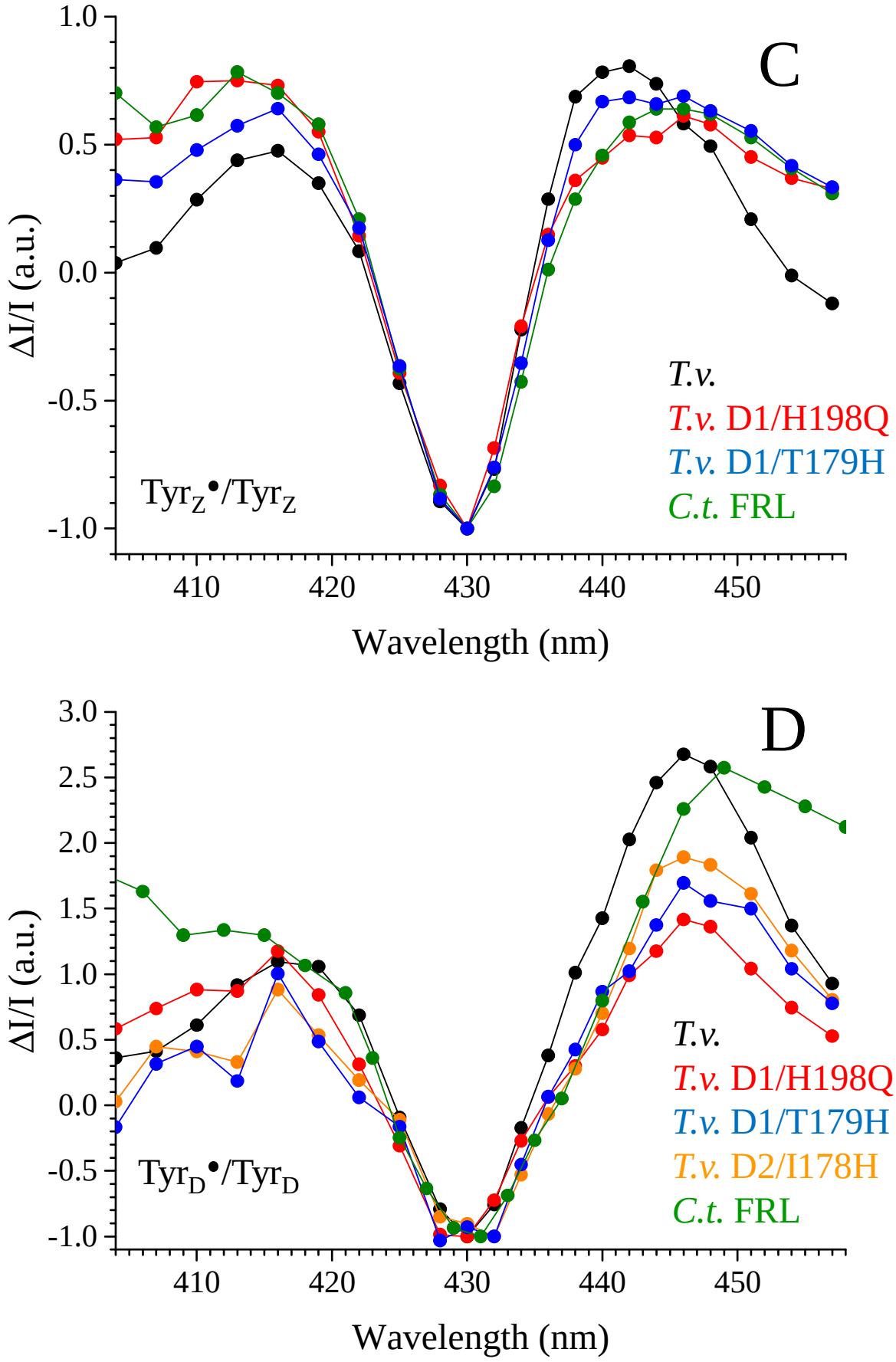
C
1.0
0.5
0.0
-0.5
-1.0
ΔI/I (a.u.)
410
420
430
440
450
Wavelength (nm)
Tyr$_Z$•/Tyr$_Z$
T.v.
T.v. D1/H198Q
T.v. D1/T179H
C.t. FRL
D
3.0
2.5
2.0
1.5
1.0
0.5
0.0
-0.5
-1.0
ΔI/I (a.u.)
410
420
430
440
450
Wavelength (nm)
Tyr$_D$•/Tyr$_D$
T.v.
T.v. D1/H198Q
T.v. D1/T179H
T.v. D2/I178H
C.t. FRL

Fig. 5

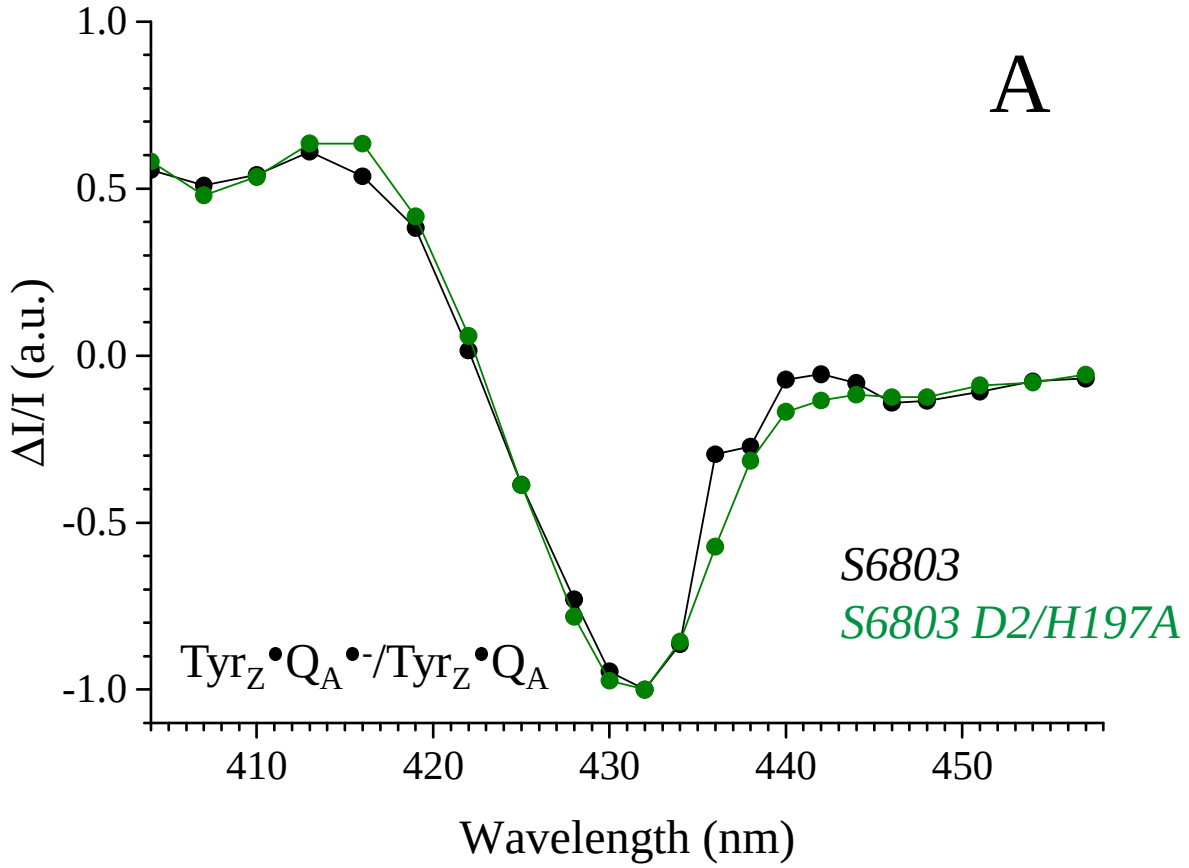
A
1.0
0.5
0.0
-0.5
-1.0
ΔI/I (a.u.)
410
420
430
440
450
Wavelength (nm)
S6803
S6803 D2/H197A
TyrZ•QA•-/TyrZ•QA

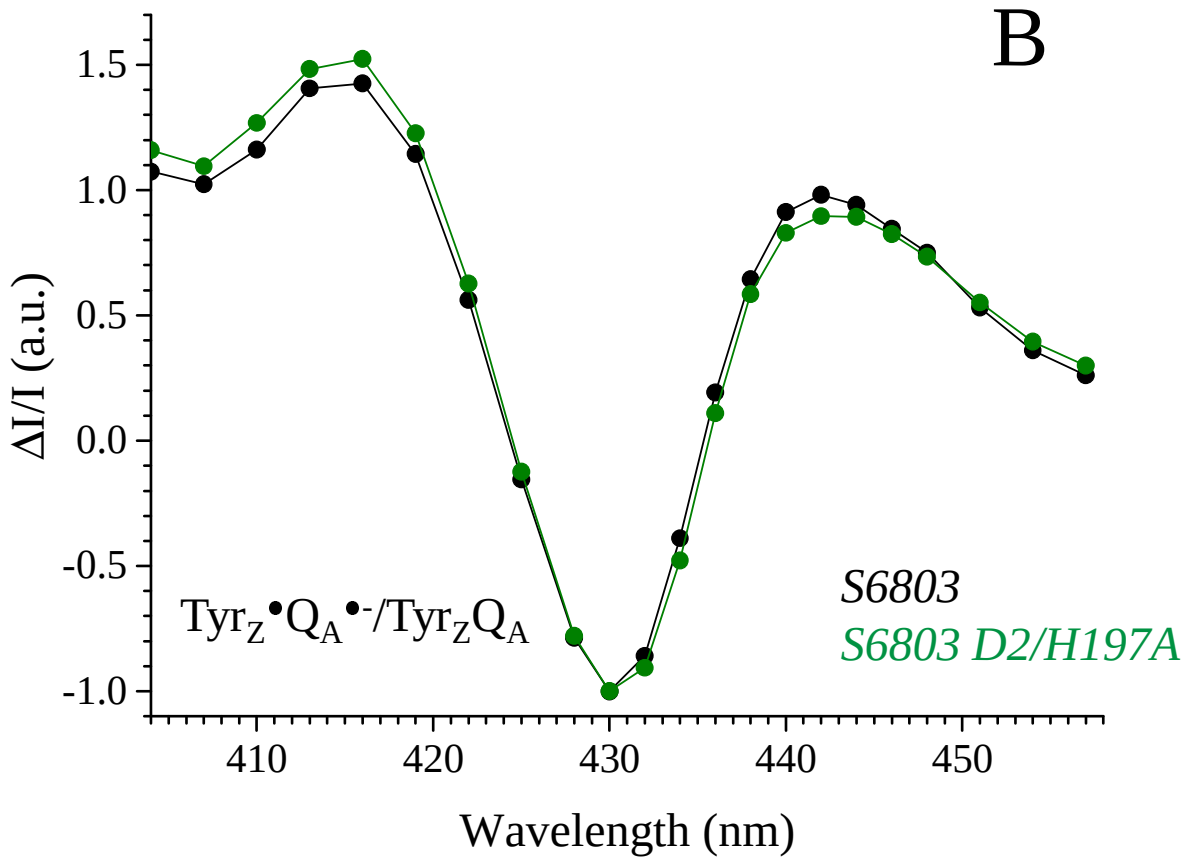
B
1.5
1.0
0.5
0.0
-0.5
-1.0
ΔI/I (a.u.)
410
420
430
440
450
Wavelength (nm)
S6803
S6803 D2/H197A
TyrZ•QA•-/TyrZQA

Fig. 6

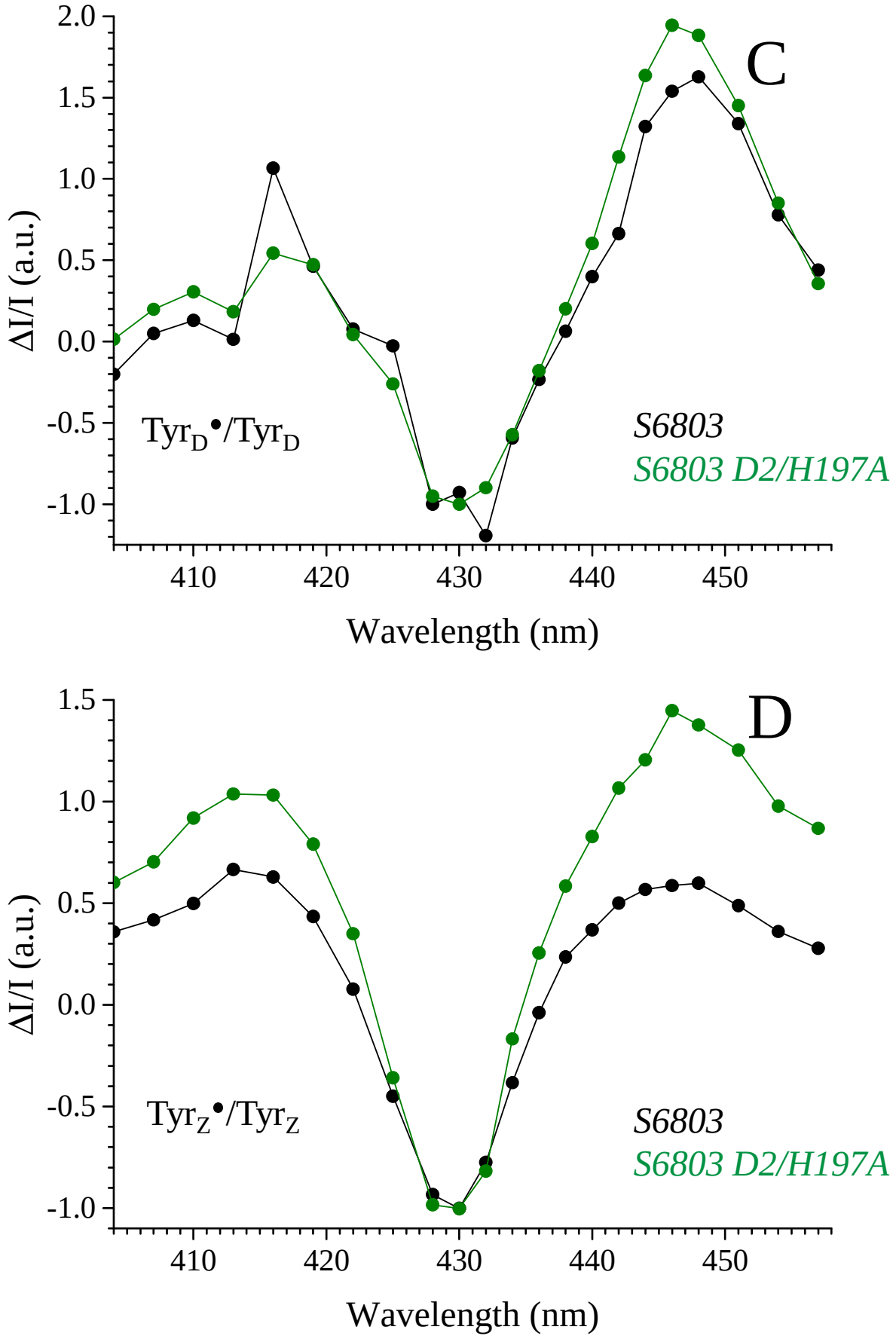
C
2.0
1.5
1.0
0.5
0.0
-0.5
-1.0
ΔI/I (a.u.)
Tyr$_D$•/Tyr$_D$
S6803
S6803 D2/H197A
410
420
430
440
450
Wavelength (nm)
D
1.5
1.0
0.5
0.0
-0.5
-1.0
ΔI/I (a.u.)
Tyr$_Z$•/Tyr$_Z$
S6803
S6803 D2/H197A
410
420
430
440
450
Wavelength (nm)

Fig. 6

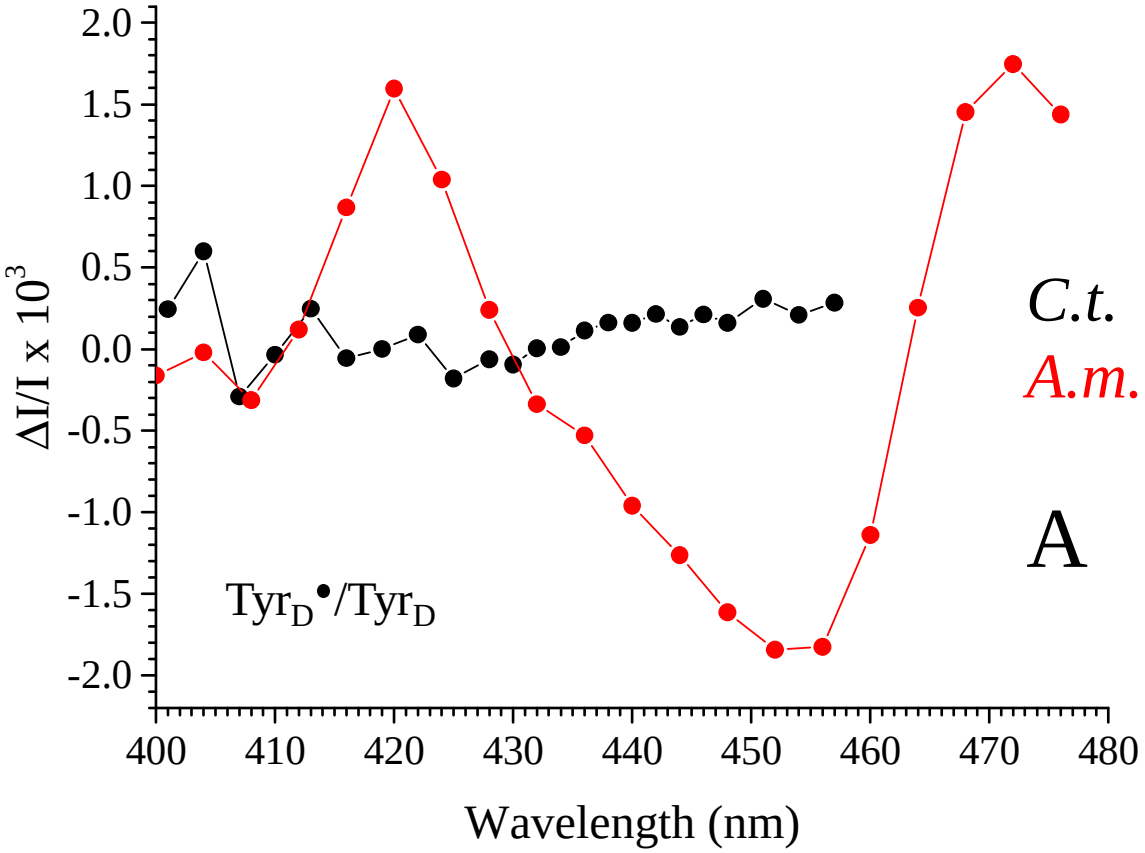
2.0
1.5
1.0
0.5
0.0
-0.5
-1.0
-1.5
-2.0
ΔI/I x 10^3
400
410
420
430
440
450
460
470
480
Wavelength (nm)
C.t.
A.m.
A
Tyr_D•/Tyr_D

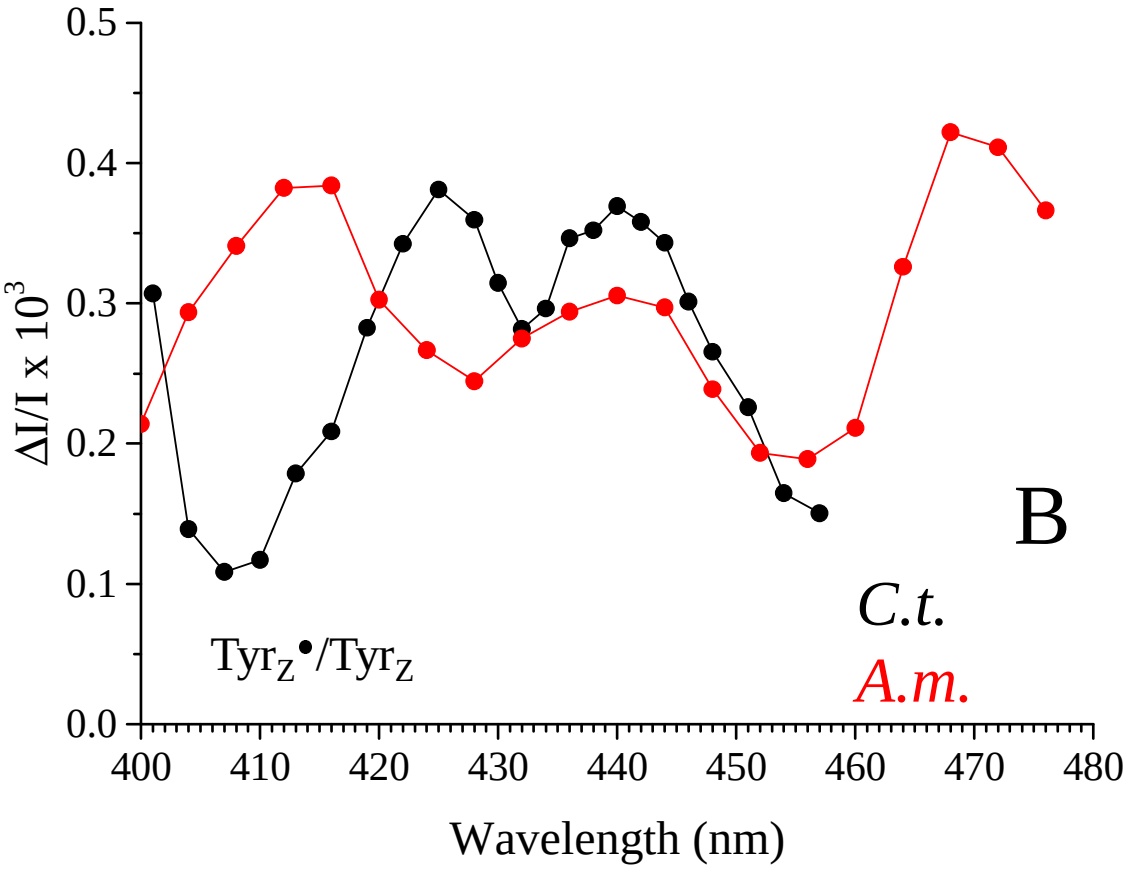
0.5
0.4
0.3
0.2
0.1
0.0
ΔI/I x 10^3
400
410
420
430
440
450
460
470
480
Wavelength (nm)
B
C.t.
A.m.
Tyr_Z•/Tyr_Z

Fig. 7

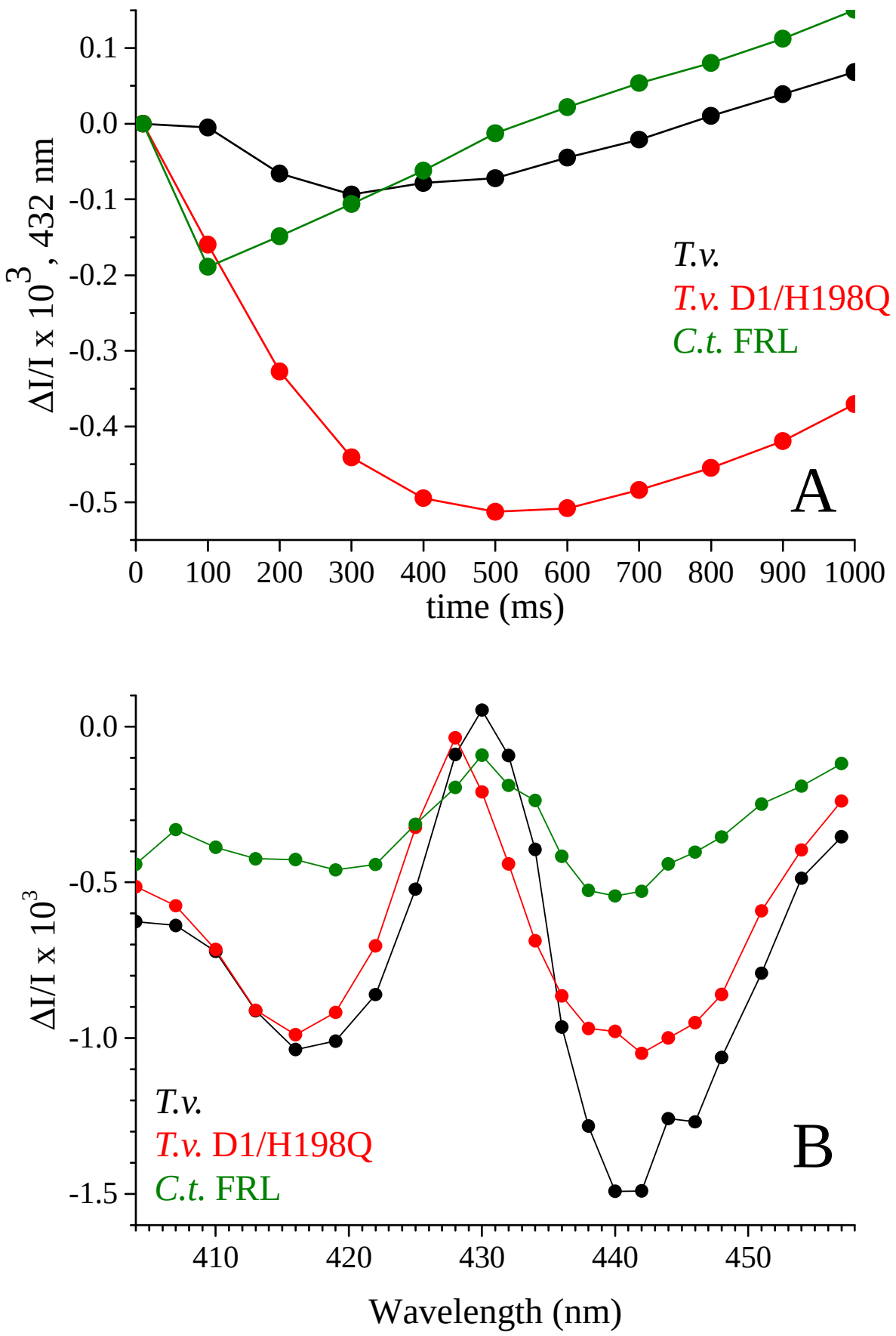
0.1
0.0
-0.1
-0.2
-0.3
-0.4
-0.5
ΔI/I x 10^3, 432 nm
0
100
200
300
400
500
600
700
800
900
1000
time (ms)
T.v.
T.v. D1/H198Q
C.t. FRL
A
0.0
-0.5
-1.0
-1.5
ΔI/I x 10^3
410
420
430
440
450
Wavelength (nm)
T.v.
T.v. D1/H198Q
C.t. FRL
B

Fig. 8